Indian Journal of Science and Technology, *Vol 9(46), DOI: 10.17485/ijst/2016/v9i46/107494, December 2016*
ISSN (Print) : 0974-6846
ISSN (Online) : 0974-5645

Analysis of Temperature Fields Distribution in the Technological Tooling for Transfer Molding

Dmitry Golovatov*[1], Maxim Mikhaylov[1] and Aleksey Bosov[2]

[1]The Bauman Moscow State Technical University, Moscow, Russia; gda.mgtu@mail.ru, mms.mgtu@mail.ru
[2]Materials Processing Technology Ltd; bav.tpm@mail.ru

Abstract

Objectives: Distribution of temperature fields in technological tooling for transfer molding of carbon fiber composite load-bearing rod elements has been studied in this article. **Methods:** Computational study has been conducted by finite element analysis. Specific features of simulation of heat flows, temperature and deformation fields distribution in the model of compound tooling and carbon perform, impregnated with polymeric matrix, were described. **Findings:** It was studied how thermal deformations of composite tooling can affect the dimensional precision of the manufactured composite rods. **Improvements:** The results of calculations are used for evaluation the uniformity of temperature fields in the preform and tooling in the process of polymeric matrix curing.

Keywords: Accuracy of Manufacture, Carbon Fiber Curing, Finite Element Analysis, Transfer Molding, Technological Tooling

1. Introduction

Creation of large space structures is associated with the solution of a number of technical optimization problems, due to the uniqueness of designed objects. A characteristic feature of such problems is a combination of requirements for increasing of dimensions and providing sufficient stiffness in response to minimization the weight of load-bearing structure. To meet these requirements high modulus carbon fiber reinforced plastics are used in the structures.[1,2] Typically, such structures are launched into orbit in the folded transport condition and their further set-up is driven by implementation of the process of opening. In series of such structures opening is provided through the use of telescopic booms, which consist of carbon fiber composite load-bearing rod elements. One of the manufacturing methods of composite load-bearing rod elements is transfer molding. The process of transfer molding involves feeding of resin into closed preform cavity under pressure.[3] The cost of tooling for transfer molding significantly exceeds the cost of tooling used in alternative methods of composite products moulding.[4,5] Nevertheless the manufacturing process of transfer moulding allows providing mass production of high quality products with the minimum possible to date characteristic spread of the composite products. However, optimization of transfer molding and subsequent curing of composite products requires a large amount of experimental and theoretical studies with the aim to eliminate possible technological imperfections. To ensure quality of designed composite products in the present study we have investigated distribution of temperature fields in technological tooling for transfer molding.[6–8]

In this field studies have been conducted directed to calculation of relationship between temperature of the mold and deformations under temperature control of the mold by electric heating and water cooling.[9] Also the studies of tooling deformations for sand casting under

*Author for correspondence

action of iron casting expansion since the beginning of hardening at 200°C were conducted.[10] The studies of thermal stability of the mold, which includes inorganic matrix and filler with high heat resistance and low thermal expansion, were conducted.[11] Many studies of pressure die casting are also focused on cooling channels, which have different shape and cross section, and optimization of the cross section is conducted for the best preform cooling.[12]

2. Concept Headings

Investigations of temperature field distribution in technological tooling for transfer molding are conducted with the help of engineering review by finite element analysis.

Engineering review represents a complex of tests, designed for assessment of ability of equipment, structures and also products produced to bear a project load and to work at rated duty.

In modern design various program packages of Computer-Aided Engineering (CAE) are widely used, which allow to conduct engineering review of computer models without real experiments.

CAE is a common name for programs and program packages designed for solution of different engineering tasks: calculations, analysis and simulation of physical processes. Calculation part of program packages typically is based on numerical computation of differential equations (finite element analysis, finite volume method, finite difference method, etc.).

CAE systems represent a variety of program products, which allow assessing with the help of calculation methods how the product computer model will behave under actual operating conditions. These systems help to ensure product working capacity without heavy spending of time and money.

Most common and effective calculation method, applied in CAE systems is a Finite Element Analysis (FEA). Systems which use FEA as numerical analysis of technical constructions are called FEA systems.

Modern CAE are used together with CAD systems and often are integrated in them. In this case they are called hybrid CAD/CAE systems.

Overview of FEA

Analysis by FEA starts with digitalization of the region of interest (task area) and its compartition into cells of a mesh. Such cells are called finite elements (FE).

FE may have different shape. In contrast to real construction FE in discrete model are connected together only in isolated points (nodes) determined by finite amount of nodal parameters.

Selection of suitable elements with necessary amount of nodes from the library of accessible elements is one of the most important decisions for a user of FEA package. Designer also must set a total amount of elements (their size in other words).

FEA classical form is known as h-version. Piecewise polynomials of constant degrees are used in this method as a shape function and accuracy is increased through decrease of the cell size. The p-version uses a fixed mesh and accuracy is increased through increase of the shape function degree. Common rule is that the more amount of nodes and elements (в h- version) or the higher shape function degree (p-version), the solution is more accurate, but more expensive from calculation point of view.

The next step is assembling. Assembling is a combination of individual elements into finite element mesh. From a mathematical standpoint assembling consists in assembly of rigidity matrixes of single elements into one global rigidity matrix of entire construction. In this case two numbering systems of element nodes are fundamentally used: local and global. Local numbering is a constant nodal numbering for each type of FE in accordance with introduced local coordinate system on the element. Global nodal numbering of entire construction may be absolutely random, as well as global numbering of FE. However one-to-one correspondence exists between local numbers and global numbers of nodes, on the base of which global system of finite element equations is formed.

Approximation

FEA refers to discrete analysis methods. However in contrast to numerical methods based on mathematical digitalization of differential equations, FEA is based on physical digitalization of object being examined. Real construction as continuous medium with a lot of infinite number of degrees of freedom is replaced by discrete model of interconnected elements with finite number of degrees of freedom. Since possible number of discrete models for continual region is infinitely large, the major task consists in selection of the model that approximate this region best of all.

Subject matter of continuous medium approximation by FEA is as follows:

1. Region of interest is divided into certain number of FE and family of elements across the region is named the system or FE mesh;
2. It is expected that FE are connected together in finite number of points – nodes, situated along the outline of each FE;
3. Polynomial approximant is set for each FE.

Approximating functions:

Polynomial approximant for one-dimensional FE:

$$u(x) = \sum_{i=0}^{r} a_i x^i$$

Example for one-dimensional FE:

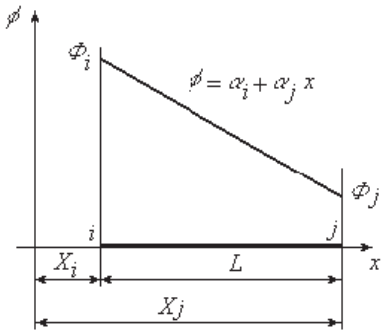

Example for two-dimensional FE:

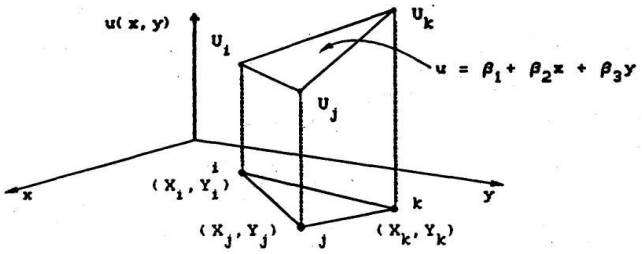

Polynomial approximant of the second order:

$$u^e(x,y) = \beta_1 + \beta_2 x + \beta_3 y + \beta_4 x^2 + \beta_5 xy + \beta_6 y^2$$

Polynomial approximant degree defines number of nodes for each element. It should be equal to the number of unknown coefficients α_i, included into polynomial.

Required functions within each FE (for example, distribution of displacements, deformations, strains, etc.) are expressed with the help of approximating functions through nodal values, which represent main unknown FE.

Required approximating function:

$$u(\bar{x}) = \sum_{i=0}^{r} h_i(\bar{x}) q^i$$

Where: h(x) = co-ordinate /basic functions, so called shape function;

q = unknown coefficients (nodal values).

In matrix view:

$$\overline{U}(\bar{x}) = \overline{H}\,\overline{U}$$

Approximation usually gives approximate but not exact description of real distribution of required values in the element. Because of that the results of structural analysis in the general case are also approximate. Naturally a question of accuracy, stability and convergence of solutions, obtained by FEA may be posed.

Accuracy is understood as deviation of approximate solution from accurate or true solution. Stability first of all is defined by error growth while performing certain computing operations. Unstable solution is a result of the wrong choice of approximating functions, "bad" region dividing, incorrect representation of the boundary conditions, etc. Convergence is understood as gradual approximation of successive solutions to ultimate solution as long as parameters of discrete model are determined, such as element dimensions, degree of approximating function, etc. In this regard the concept of convergence is similar to the meaning that it has in usual iteration processes. Therefore in converging procedure difference between consequent solutions is decreased, approaching zero at the extreme.

Abovementioned concepts are illustrated in Figure 1. Herein x-axis defines degree of clarification of parameters of discrete model, and y-axis defines approximate solution obtained at that clarification. In the figure the monotonic type of convergence is shown, at which solution accuracy is smoothly increased.

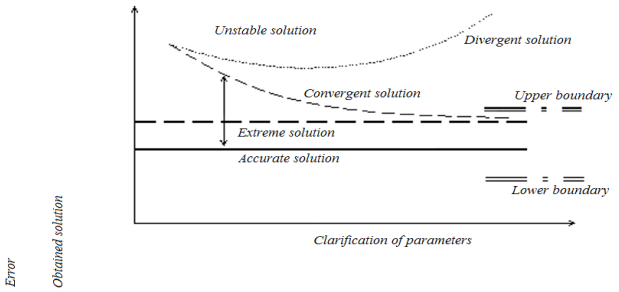

Figure 1. Dependence of solution from parameters.

Setting of boundary conditions and material

After task area approximation by the set of discrete finite elements we should define materials characterization and boundary conditions for each element. With the indication of different characteristics for different elements, we can analyze behavior of an object composed of different materials.

According to terminology of mathematical physics that considers various differential equations describing physical fields from unified mathematical point of view, boundary or edge conditions for given differential equations are divided into two basic types: essential and natural. Usually essential conditions are imposed on required function and natural ones are imposed on its spatial derivatives.

From the standpoint of FEA essential boundary conditions are such that shape the model degrees of freedom and are imposed upon components of global vector of unknown U (displacements). Alternatively natural boundary conditions are such that indirectly influence on degrees of freedom through the global system of finite-element equations and are imposed on right part of the system – vector F (applied forces).

As a rule essential boundary conditions in mechanical tasks are such that include displacements (but not deformations, representing space derivative of displacements). According to terminology of the theory of elasticity such boundary conditions are known as kinematic. For example, embedding and hinge support in rod tasks are essential or kinematic boundary conditions, imposed on a bend or longitudinal displacements of the rod points. Notice that in rod bending tasks essential boundary conditions are also conditions, imposed on a first derivative of the rod bending on axial coordinate that has mechanical sense of angle of the rod rotation. The same may be said about angle of rotation in the plate bending theory.

Natural boundary conditions in mechanical applications of FEA are conditions, imposed on different external force factors affecting points of the body's surface – concentrated forces and moments in rod tasks, distributed forces in two-dimensional and three-dimensional tasks. Such restrictions are called force boundary conditions.

Mixed boundary conditions are widely used in setting objectives of continuum mechanics particularly in the theory of elasticity. It means that some components of displacements and surface forces are simultaneously set in this point of the body's surface.

Three enumerated variants of boundary conditions are the most widespread in pure mechanical applications of FEA.

Besides boundary conditions for resolving of equations it is necessary to set characterization of material of which research object is made. For example, in stress-strain analysis parameters determine connection of tension and deformation.

System of equations forming

After set up of the boundary conditions and material, FEA program forms a system of equations, connecting the boundary conditions with unknowns, whereupon solve the system against unknowns.

Result generation

After finding of values of unknowns user gets a possibility to calculate value of any parameter in any point of any FE by the same required function that was used for system of equations forming. FEA program outputs are usually presented in a numerical form. However it may be difficult to get general picture about behavior of corresponding parameters from numeric data. Graphic images are more informative usually, because they give an opportunity to study behavior of parameters over the whole task area.

FEA Formulation

By means of getting basic, i.e. resolving equations, there are four main kinds of FEA: direct, variational, weighted residuals and energy balance. Among enumerated kinds of FEA variational method and weighted residuals Galerkin method are particularly topical in structural mechanics.

Let us consider the variational method. This method is based on stationary principle of some variable that depends on one or more functions (such variable is named functional). In respect to mechanics of deformable solids this variable represents potential (Lagrangian functional) or additional (Castigliano's functional) energy of the system or is formed on the basis of these two energies (Hellinger-Reissner and Hu-Washizu functionals). If substitute approximating expressions of the required functions into functional and apply extremum principles (accordingly Lagrange principle, Castigliano's principle, etc.) to it, we will get the system of algebraic equation, the solution of that will be values of nodal unknowns.

Variational Lagrange principle: potential energy acquires stationary values on kinematically admissible displacements, which satisfy specified boundary conditions and force equilibrium conditions.

In contrast to direct method, variational method can in equal measure be successfully applied to both simple and challenging tasks.

So let us consider three-dimensional object of arbitrary shape, being in equilibrium condition affected by some stress load (Figure 2). Let us denote friction forces affecting the surface (surface forces) by p, and mass forces (volume forces) – by G. In general these forces are laid out on components parallel to the axes of coordinates:

$$G = \begin{bmatrix} G_x \\ G_y \\ G_z \end{bmatrix} p = \begin{bmatrix} p_x \\ p_y \\ p_z \end{bmatrix} \quad (1)$$

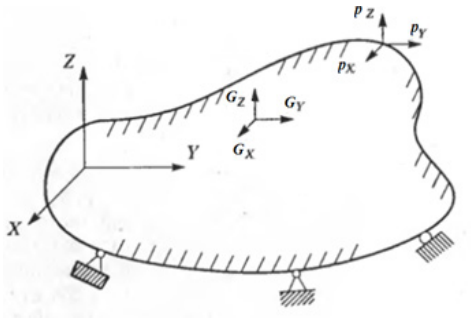

Figure 2. Three-dimensional object with external forces.

Let us denote displacement of arbitrary point of the object (X,Y,Z) in comparison with configuration in absence of stress load by symbol U. In this case

$$U^T = [U(X,Y,Z) \cdot V(X,Y,Z) \cdot W(X,Y,Z)] \quad (2)$$

Displacements U will lead to occurrence of deformation

$$\varepsilon^T = [\varepsilon_{XX} \cdot \varepsilon_{YY} \cdot \varepsilon_{ZZ} \cdot \varepsilon_{XY} \cdot \varepsilon_{YZ} \cdot \varepsilon_{ZX}] \quad (3)$$

and relevant strains

$$\sigma^T = [\sigma_X \cdot \sigma_Y \cdot \sigma_Z \cdot \tau_{XY} \cdot \tau_{YZ} \cdot \tau_{ZX}] \quad (4)$$

It is necessary to calculate U, ε, σ in the point (X,Y,Z) with respect to preset external forces. Total potential energy of elastic body is described by expression:

$$\ddot{I} = \dot{Y} - \dot{A} = \frac{1}{2} = \int_V \bar{\varepsilon}^T \sigma dV - \int_V \overline{U}^T G dV - \int_S \overline{U^S}^T p dS \quad (5)$$

Where Э = energy of deformation;
A = work of applied mass and surface forces.

Three last items of equation (5) describe the external work, executing by real forces G, p on virtual displacements $\overline{U}$.

A superscript S of vector $\overline{U}$ means virtual displacement on the surface. Strains are calculated through deformations by relevant constitutive equations.

Let us obtain FEA equations from equation (5), starting with approximation of the object represented in Figure 2 by FE mesh. Elements are connected together in nodal points which are located on their boundaries. Displacement in any point with coordinates (x, y, z) in the local coordinate system of element is considered a function of displacements in nodal points.

So for the element T assumption is declared that

$$u^{(m)}(x,y,z) = H^{(m)}(x,y,z)\overline{U} \quad (6)$$

Where H = interpolation displacement matrix (shape functions), $\overline{U}$ = vector of displacement on all nodes. If total amount of nodes is equal N, vector $\overline{U}$ is written as follows:

$$\overline{U}^T = [u_1 \upsilon_1 w_1 u_2 \upsilon_2 w_2 \ldots u_N \upsilon_N w_N] \quad (7)$$

This expression can be rewritten as:

$$\overline{U}^T = [U_1 U_2 \ldots U_n] \quad (8)$$

Although displacements of all nodes are specified in equation (8) and therefore these displacements are also included into expression (6), for each certain element internal displacements are determined by displacements in its nodes only. All nodes have entered into expression (6) because it facilitates the process of combination of matrix of single elements into matrix of structure in whole, as it will be shown below.

Equation (6) allows calculating of deformations:

$$\varepsilon^{(m)}(x,y,z) = B^{(m)}(x,y,z)\overline{U} \quad (9)$$

Rows of a matrix deformations-displacements $B^{(m)}$ from equation (9) are obtained by differentiation and combination of matrix rows $H^{(m)}$.

Now we can also write expressions for strains inside each element:

$$\sigma^{(m)} = C^{(m)}\varepsilon^{(m)} + \sigma_0^{(m)} \quad (10)$$

Where C = flexibility matrix of element T (Hooke matrix), $\sigma_0^{(m)}$ = initial strain inside the element. In

structure of different elements it is possible to preset own flexibility matrix for each of them.

Let us rewrite equation (5) in view of sum of volume integrals and integrals over the surfaces of single elements:

$$\bar{I} = \sum_m \bar{I}^{(m)} = \frac{1}{2}\sum_m \int_{V^{(m)}} \overline{\varepsilon^{(m)}}^{\partial} \sigma^{(m)} dV^{(m)} - \sum_m \int_{V^{(m)}} \overline{u^{(m)}}^T G^{(m)} dV^{(m)} - \sum_m \int_{S^{(m)}} \overline{u^{S(m)}}^T p^{(m)} dS^{(m)} \quad (11)$$

Where element T varies from 1 to total amount of elements in the system.

Substitution of (6), (9) and (10) into (11) will give the next expression:

$$\sum_m \bar{I}^{(m)} = \frac{1}{2}\sum_m \int_{V^{(m)}} B^{(m)T} \overline{U}^T C^{(m)} B^{(m)} \overline{U} dV^{(m)} - \sum_m \int_{V^{(m)}} H^{(m)T} \overline{U^T} G^{(m)} dV^{(m)} - \sum_m \int_{S^{(m)}} H^{S(m)T} \overline{U^T} p^{(m)} dS^{(m)} + \sum_m \int_{V^{(m)}} \sigma_0^{(m)} B^{(m)T} \overline{U^T} dV^{(m)} \quad (12)$$

Where surface interpolation matrixes of displacements $H^{S(m)}$ are obtained from volume interpolation matrixes of displacements $H^{(m)}$ by substitution of coordinates of element surface.

Let us denote

$$K = \sum_m \int_{V^{(m)}} B^{(m)T} C^{(m)} B^{(m)} dV^{(m)} \quad (13)$$

$$R = R_B + R_S - R_0 \quad (14)$$

$$R_B = \sum_m \int_{V^{(m)}} H^{(m)T} G^{(m)} dV^{(m)} \quad (15)$$

$$R_S = \sum_m \int_{S^{(m)}} H^{S(m)T} p^{(m)} dS^{(m)} \quad (16)$$

$$R_0 = \sum_m \int_{V^{(m)}} \sigma_0^{(m)} B^{(m)T} dV^{(m)} \quad (17)$$

Energy minimization Π results in equation:

$$\frac{\partial \bar{I}}{\partial U} = \frac{\partial}{\partial U} \sum_m \bar{I}^{(m)} = 0 \quad (18)$$

which with account of introduced notations will be written as:

$$KU = R \quad (19)$$

Note that summing of integrals taken over volumes of single elements in formula (14) expresses the fact that rigidity matrix of set of elements as a whole is obtained by addition of rigidity matrix of elements $K^{(m)}$. Similarly vector R_B of volume force, affecting the whole body, is obtained by summing of volume force vectors, affecting separate elements. Vectors of other forces are calculated in the same way.

The expression (19) describes static equilibrium. When applied forces are varying with time, this expression is applicable to any certain moment. However on rapid loading inertial forces must be considered. On the d'Alambert's principle inertial forces of single elements may be added to mass forces. If we assume that acceleration in any point of the element is connected to acceleration in nodal points by matrix $H^{(m)}$ alike displacements, input of mass forces into force vector K will be expressed as:

$$R_B = \sum_m \int_{V^{(m)}} H^{(m)T} [G^{(m)} - \rho^{(m)} H^{(m)} \ddot{U}] dV^{(m)} \quad (20)$$

Where $\ddot{U}$ = accelerations in nodal points, and $\rho^{(m)}$ = mass density of element T.

Substitution of (20) instead of (15) into (19) will give a new equilibrium equation:

$$M\ddot{U} + KU = R \quad (21)$$

Where M = mass matrix.

Note that U and R in equation (21) are time functions.

Damping forces may be taken into account as additional input into mass forces, that allow describing damping effect (attenuation). In this case the equation (20) takes a new form:

$$R_B = \sum_m \int_{V^{(m)}} H^{(m)T} [G^{(m)} - \rho^{(m)} H^{(m)} \ddot{U} - k^{(m)} H^{(m)} \dot{U}] dV^{(m)} \quad (22)$$

Where $\dot{U}$ = velocity vector of nodal points, and $k^{(m)}$ = damping coefficient for element T.

The equilibrium equation takes the form of

$$M\ddot{U} + C\dot{U} + KU = R, \quad (23)$$

Where C = damping matrix.

In practice matrix C is usually constructed from mass matrix and rigidity matrix on the grounds of experimental data on damping in material, because it is quite difficult to define damping parameters of single elements.[14–16]

Further the order of simulation of impregnation of load-bearing rod elements of transformable guy-roped reflectors by transfer molding is described.

For study of distribution of temperature fields in technological tooling for transfer molding it is necessary to develop geometric models of elements of composite tooling and geometric model of carbon

preform impregnated by polymer matrix. After that it is necessary to conduct partitioning of geometric models into FE and to set thermophysical and strain-stress characteristics of materials of models and further to set the boundary conditions, carry out thermal calculation and analyze findings.

2.1 Geometric Model

For carrying out thermal calculations the constructed geometrical model has been simplified because geometrically complex structural elements not significantly affect the results, but significantly affect the estimate time. All comparatively small-size details, chamfers, fillets were eliminated from the model.

A computational scheme of load-bearing rod element is presented in Figure 3, where q_c is convective heat flow. This model consists of a mandrel 1 on which at certain angles a carbon ribbon is wound forming the preform 2. The mandrel with the wound preform 2 is fit in silicone filler 3 and in collecting box 4 with end caps 5.

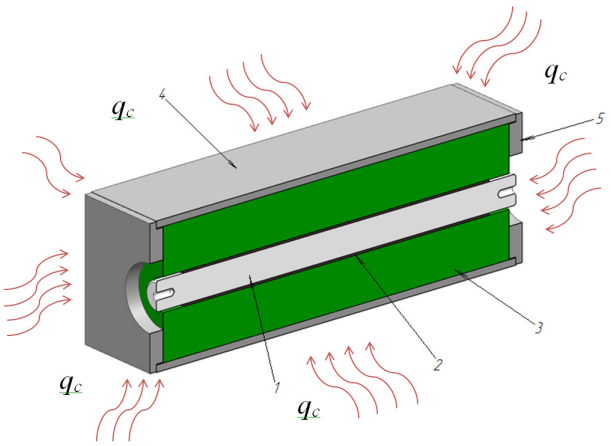

Figure 3. Calculation matrix model of size 270Ч20Ч20 mm.

2.2 Simulation of Thermal State of the Tooling Models.

Thermal impact on tooling is conducted in a convection oven. Conditions of thermal loading were approximated by applied convection thermal flow with a capacity close to capacity of the oven. The flow distribution was accepted symmetrical relating to the zero horizontal plane. Characteristics of the thermal loading are given in Table 1. The total exposure time was taken equal to $1.12 \cdot 10^5$ s, which is enough to warm all elements of the construction up to maximum temperature according to calculations. The temperature loading mode is shown in the diagram (Figure 2).

Table 1. Thermal impact

Time, s	Coefficient of convection, W/(m²·°C)	Temperature, °C
0	3.55	55.00
3600	3.55	55.00
3780	4.57	80.00
90180	4.57	80.00
90480	6.25	120.00
94080	6.25	120.00
112080	6.25	120.00

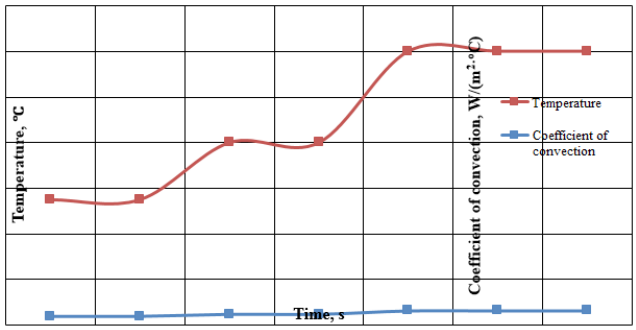

Figure 4. Diagram of temperature loading mode.

Such values of heat flow and temperature loading mode were due to the properties of the used polymer matrix that requires a strictly defined mode of curing.[13]

In the simulation process of heat transfer the following assumptions were accepted:

- The materials used were considered solid and homogenous;
- Chemical composition and physical state of the material were considered unvaried in the process of analysis;
- Phisical characteristics such as density, heat capacity and thermal conductivity were assumed constant without consideration anisotropy of properties of specified materials.

For two parts of the box 4, end caps 5 and silicone filler 3 material properties of steel СТ13сп GOST 4784-97 and silicone were specified respectively. For cylindrical mandrels 1 material properties of

aluminium D16T GOST 4784-97 have been determined. It was assumed that the thermophysical properties of impregnated preform do not change depending on temperature loading mode. Basic materials employed and their thermophysical properties are presented in Table 2.

Table 2. Thermophysical properties of basic materials employed

Material	Density, kg/m^3	Thermal capacity, J/(kg·K)	Thermal conductivity, W/(m·K)
Aluminium D16T GOST 4784-97	2640	922	122
Silicone	1750	1200	0.17
Carbon fiber M46J Torayca	1510	1120	30

2.3 FE Mesh Building

In the process of solution FE mesh was built by two different methods: automatic and adaptive. Automatically generated FE mesh had mesh elements of large size and irregular distribution of elements by model volume. Figure 3 shows FE mesh generated by automatic method. In building of adaptive FE mesh such methods as Sweep method and stretching method were used. Sweep method generates a mesh by stretching mesh elements along the model of the body. Scr/TrgSelection function was chosen in this method, allowing to select manually the initial and final plane for stretching FE mesh. For other elements of the matrix model a stretching method was applied. Stretching method is what a 2D mesh is formed on one of the faces and is stretched along the body by use of step, thereby forming 3D mesh. Through the use of these methods of FE mesh building, well-ordered structured mesh was generated with regular arrangement of elements and minimum amount of disproportional inclusions, at that the size of the mesh element reached 2 mm, which allowed to conduct more accurate calculation. FE mesh built by adaptive methods in volume of the tooling model is presented in Figure 4 in diagram form. The number of elements in resulting meshes is presented in comparison Table 3.

Table 3. Comparison table of FE number of relevant models

No. of calculation model	FE number of relevant models	
	Automatic method	Adaptive method
1	7411	568138
2	7636	526580
3	9009	554397
4	19101	1271901

Automatic method of the mesh building

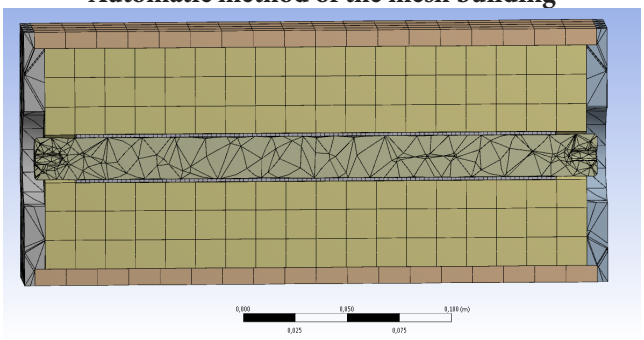

Figure 5. Automatic FE mesh of tooling model of size 270Ч20Ч20 mm.

Adaptive method of the mesh building

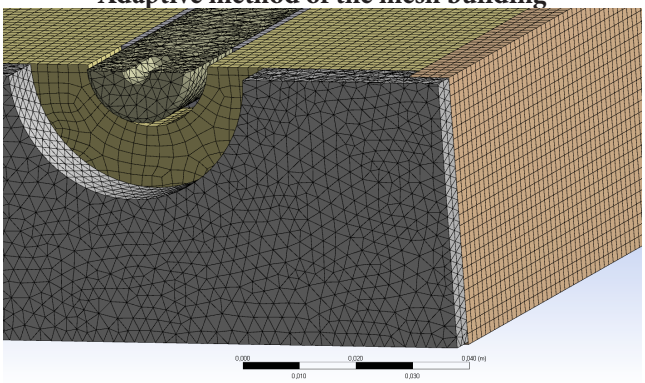

Figure 6. Adaptive FE mesh of tooling model of size 270Ч20Ч20 mm.

2.4 Analysis of Tooling for Distribution of Heat Flows

Material from table 2 for the built tooling model (Figure 1) and for the mesh generated in it (Figure 4) was specified and heat loading was applied in the form of convective thermal loading with values and mode from table 1.

3. Results

Findings of conducted analysis are distribution of temperature and heat flows through the body of the model. Table 4 shows maximum and minimum temperature and heat flows at characteristic points of temperature mode. Figure 5 shows a diagram of maximum and minimum temperature distribution, depending on the loading mode. Figure 6 shows a diagram of heat flow distribution depending on the loading mode.

Table 4. Comparison table of temperature distribution through the body of matrix models

	Tooling model of size 270Ч20Ч20 mm Temperature, °C		Tooling model of size 270Ч20Ч20 mm Thermal flow, W/m²	
Time, s	max	max	max	min
1120.8	34.464	915.92	915.92	0.30
2241.6	39.236	942.35	942.35	0.16
5604	63.124	1175.30	1175.30	$8.17 \cdot 10^{-2}$
15691	75.311	298.29	298.29	0.13
26899	78.725	97.23	97.23	$1.90 \cdot 10^{-2}$
38107	79.648	29.98	29.98	$2.83 \cdot 10^{-3}$
49315	79.902	8.76	8.76	$2.30 \cdot 10^{-3}$
60523	79.973	2.49	2.49	$9.30 \cdot 10^{-4}$
71731	79.992	0.70	0.70	$2.38 \cdot 10^{-4}$
82939	79.998	0.19	0.19	$2.39 \cdot 10^{-5}$
94147	114.950	494.66	494.66	$4.02 \cdot 10^{-2}$
105360	118.940	102.08	102.08	$4.74 \cdot 10^{-2}$
112080	119.650	41.14	41.14	$8.57 \cdot 10^{-3}$

Temperature distribution in section of tooling model of size 270Ч20Ч20 mm

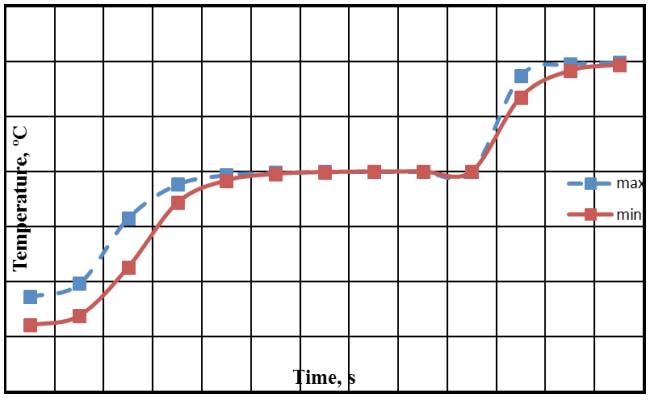

Figure 7. Diagram of temperature distribution in the body of model according to thermal mode.

Heat flow distribution in section of matrix model of size 270Ч20Ч20 mm

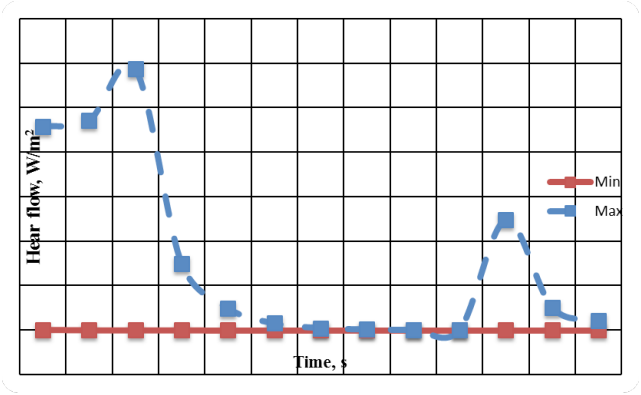

Figure 8. Diagram of heat flow distribution in the body of model according to thermal mode.

4. Discussion

Present studies were conducted for transfer molding tooling and were aimed at the study of deformations in it, whose can affect the dimensions of load-bearing rod elements for transformable aerial reflectors. The uniqueness of this study lies in the fact that the tooling is made from alloy D16T GOST 4784-97 and has low cost.

5. Conclusion

As a result of conducted analysis it was found that deformations arising in the process of heat transfer in the volume of the mandrel are in the range of 10^{-1} to 10^{-2} mm, and therefore such deformations will not lead to a significant deviation of dimensions of the produced carbon fiber rod.

Moreover it was shown that the calculated values of temperature gradients in the volume of the mandrel are not significant, therefore the curing process of the polymer matrix will be uniform by volume of the material that determines high quality of the final composite rod.

According to results of the conducted analysis it may be concluded that in relevant mandrel models the temperature is distributed from the ends to the middle part. Such a heating effect is due to the fact that the ends of the mandrels are in direct contact with the convection heat flows generated by the oven, while the middle part is located in the inner cavity of the tooling, consisting of three different materials, thermophysical properties of which are different.

6. Acknowledgments

This work was supported in part by the Ministry of Education and Science of the Russian Federation, subsidy agreement no. 14.577.21.0130 of October 28, 2014, unique identifier of applied research investigations no. RFMEFI57714X0130.

7. References

1. Jie J, Tuanjie L, Xiaofei M, Pei W. A nonlinear equivalent circuit method for analysis of passive intermodulation of mesh reflectors. Chinese Journal of Aeronautics. 2014 Aug; 4 (27):924–9.
2. Li T, Jiang J, Deng H, Lin Z, Wang Z. Form-finding methods for deployable mesh reflector antennas. Chinese Journal of Aeronautics. 2013; 26 (5):1276–82.
3. Chugui Y, Khalimanovich V, Verkhogliad A, Skokov D, Nakrohin I. Mechanism of telescopic spokes extension of reflector and arms. Reshetnevsky readings. 2015; 1 (19):141–3.
4. Gerasimov A, Zhukov A, Ponomarev S, Ponomarev V, Khalimanovich V. Simulation of large-scale transformable reflector with flexible spokes. Reshetnevsky readings. 2014; 1 (18):68–69.
5. William G. Frizelle Injection Molding Technology. Applied Plastics Engineering Handbook. 2nd (edn)., 2017. p. 191–202.
6. Mikheev P, Muranov A, Gusev S. Experimental definition of the module of interlayered shift of the layered carbon fiber reinforced plastic. The Bauman Moscow State Technical University. 2015.
7. Muranov A, Aleksandrov I, Buyanov I, Chydnov I, Borodulin A, Mironov Y, Nelub V. Investigation of microstructure of nanomodified polymer composite materials. Science and education. The Bauman Moscow State Technical University. 2012. p.1–10.
8. Aleksandrov I, Prosuntsov P. Determination of the Effect of Carbon Nanosized Particles on Thermophysical Characteristics of Polymer Composite Materials. Polymer Science. 2016; 9 (4):377–81.
9. Wang J, Simacek P, Advani S. Use of centroidal voronoi diagram to find optimal gate locations to minimize mold filling time in resin transfer molding. Composites Part A: Applied Science and Manufacturing. 2016 Aug; 87. p.243–55.
10. De Santis F, Pantani R. Development of a rapid surface temperature variation system and application to micro-injection molding. Journal of Materials Processing Technology. 2016 Nov; 237. p. 1–11.
11. Sozer E, Simacek P, Advani S. Resin Transfer Molding (RTM) in polymer matrix composites. Manufacturing Techniques for Polymer Matrix Composites. 2012.
12. Zhang L, Zhao G, Wang G, Dong G, Wu H. Investigation on bubble morphological evolution and plastic part surface quality of microcellular injection molding process based on a multiphase-solid coupled heat transfer model. International Journal of Heat and Mass Transfer. 2017 Jan. 104. p. 1246–58.
13. Marumotoa N, Kashimuraa H, Yoshidaa K, Toyodab T, Okanec T, Yoshidab M. Dynamic measurements of the load on gray cast iron castings and contraction of castings during cooling in furan sand molds. Journal of Materials Processing Technology. 2016 Nov. 237. p. 48–54.
14. Kim E, Cho G, Jung Y. Development of a high-temperature mold process for sand casting with a thin wall and complex shape. Thin Solid Films. September 2016.
15. Saifullah A, Masood S, Nikzad M, Brandt M. An Investigation on Fabrication of Conformal Cooling Channel with Direct Metal Deposition for Injection Moulding. Reference Module in Materials Science and Materials Engineering. 2016. ISBN-13: 978-3-659-95593-8
16. Sagdeeva Y, Kopysov S, Novikov A. Overview of Finite Element Analysis. Izhevsk, Udmurt University, 2011.